King Saud University

Arabian Journal of Chemistry

ORIGINAL ARTICLE

Cotton fabrics treated with acylhydrazone-based polyviologen to create innovative multi-stimulus responsive textiles

Rami A. Pashameah [a], Hatun H. Alsharief [a], Omaymah Alaysuy [b], Alia A. Alfi [a], Hana M. Abumelha [c], Turki M. Habeebullah [d], Nashwa M. El-Metwaly [a,e,*]

[a] Department of Chemistry, Faculty of Applied Science, Umm Al Qura University, Makkah 24230, Saudi Arabia
[b] Department of Chemistry, College of Science, University of Tabuk, 71474 Tabuk, Saudi Arabia
[c] Department of Chemistry ,College of Science, Princess Nourah bint Abdulrahman University, P.O. Box 84428, Riyadh 11671, Saudi Arabia
[d] Department of Environment and Health Research, Custodian of Two Holy Mosques Institute for Hajj and Umrah Research, Umm Al Qura University, Makkah, Saudi Arabia
[e] Department of Chemistry, Faculty of Science, Mansoura University, El-Gomhoria Street 35516, Egypt

Abstract   Novel multi-stimuli responsive cotton fibers were developed via spray-coating with an acylhydrazone-based polyviologen (AHPV). Polyviologen was prepared by supramolecular condensation polymerization of bipyridinium dialdehyde with a hydroxyl-substituted aryldihydrazide in an acidified aqueous medium. Transparent AHPV/resin nanocomposite film was deposited onto the surface of cotton fabric by well-dispersion of AHPV as a chromogenic substance in a resin binding agent. Increasing the temperature of the AHPV-coated cotton fabric from room temperature to 85 °C reversibly triggered a change in color from pale yellow (437 nm) to green (607 nm), respectively. The transparent layer immobilized onto the white cotton surface transformed into green under ultraviolet source as demonstrated by CIE Lab parameters. The photochromic impacts were explored at various AHPV. In addition, the AHPV-coated cotton immediately displayed a vapochromic activity upon exposure to $NH_{3(g)}$, and then recovered to pale yellow after removing the ammonia source away. The current AHPV-coated cotton fabric displayed a limit of detection (LOD) to $NH_{3(aq)}$ in the range of 50–150 ppm. The spray-coated cotton fabrics demonstrated a

* Corresponding author.
  E-mail addresses: n_elmetwaly00@yahoo.com, nmmohamed@uqu.edu.sa (N.M. El-Metwaly).

Peer review under responsibility of King Saud University.

Production and hosting by Elsevier

reversible photochromism, thermochromism and vapochromism with high stability. The produced AHPV nanoparticles were also studied by transmission electron microscopy (TEM), demonstrating particle diameter of 74–92 nm. The mechanical and morphological properties of the spray-coated cotton fabrics were also explored. The surface morphology of AHPV-finished samples was examined by Fourier-transform infrared (FTIR) and scanning electron microscopy (SEM). No considerable defects were observed in permeability to air and bending length of AHPV-finished samples. Additionally, high colorfastness was monitored for the AHPV-finished cotton substrates. The cytotoxic activity of the AHPV-finished cotton was also examined. Mechanistic study accounting for the multichromic activity of acylhydrazone-based polyviologen is explored.

1. Introduction

Multi-stimuli responsive materials have been able to induce colorimetric changes in response to one or more external stimuli such as light (photochromic), heat (thermochromic), and vapors (vapochromic) (Fan et al., 2020; Al-Qahtani et al., 2022a; Libanori et al., 2022). Those have been promising phenomena to create new smart materials for a variety of applications, such as protective textiles, authentication inks and early-warning sensors. Temperature-driven chromic materials have the capability to change reversibly their physical properties giving immediate colorimetric changes in response to temperature changes (Cheng et al., 2018; Hakami et al., 2022). Thermochromic materials have been employed for real-time monitoring of temperature, which is significant for products that necessitate certain temperature conditions, such as foodstuffs, vaccines, dairy and drugs (Fabiani et al., 2019; Fabiani et al., 2020; Gong et al., 2020). Additionally, temperature-driven sensors have been extended to many other applications such as smart windows (Aburas et al., 2019), foodstuff packaging (Sadoh et al., 2021), displays (Yang et al., 2019), warning signs (Xu et al., 2022), drug delivery (Gong et al., 2020), and solar control coating (Sun et al., 2018). Many smart textiles have been developed to respond to chemical, mechanical, thermal, electrical and/or light stimuli (Persson et al., 2018; Chen et al., 2020; Ramlow et al., 2021). Among them, cellulose textiles have been utilized for the development of thermochromic products (Atav et al., 2022). Polymer-finished smart textile fibers have been able to incorporate additional sensing functionalities (Oliveira et al., 2018). Viologens (1, 1′-substituted-4, 4′-bipyridinium) have been the subject of several investigations aimed to develop multi-stimuli responsive smart materials that respond to external stimuli such as chemicals, electricity, light, mechanical stress, and heat. Therefore, acylhydrazone-based polyviologens (AHPV) are suitable candidates for the development of smart materials such as sensors and molecular switches (Ding et al., 2019; Skorjanc et al., 2019). Using a reduction/oxidation process, AHPV have been employed as electrochromic devices because of their ability to reversibly change color without fatigue. Biochemical redox processes can use acylhydrazone-based polyviologens as suitable colorimetric agents. In comparison to other redox organic agents, polyviologens have been reported as highly reversible, inexpensive and very stable redox agents (Bahari et al., 2020; Blundo et al., 2021). Where, the indigenous Americans populations had been used colored fiber cotton. Viologens are materials whose properties can be reversibly switched on and off which contain redox -responsive molecule, also it is worth mentioned we have found viologen-based polymers which have several interesting properties (Li et al., 2021).

Herein, we report on the development of smart cotton fabrics with thermochromic, photochromic and vapochromic characteristics without adversely affecting on the handle, flexibility, and breathability of the cotton fabric. Cotton fabrics were chosen due to their biodegradability, high abundance, low cost and other desirable characteristics (Wang et al., 2018; Dan et al., 2020; Eid and Ibrahim, 2021). Acylhydrazone-based polyviologen was prepared by simple and environmentally friendly condensation reaction in an acidified aqueous medium. The prepared acylhydrazone-based polyviologen was spray-coated onto cotton fabrics using alkyd resin as a binding agent. Colorimetric shift from light yellow to green were monitored on the AHPV-finished textiles with increasing temperature (thermochromism) in the range of 25–85 °C, exposure to ammonia gas (vapochromism) with LOD of 50–150 ppm, and/or ultraviolet light (photochromic). As proved by CIE Lab parameters and absorption spectra, the AHPV-finished textiles exhibited two absorbance band at 437 nm (pale yellow) and 593 nm (green) under vapochromic and photochromic activities. On the other hand, two absorbance bands were detected at 607 nm (45 °C) and 514 nm (85 °C) under thermochromic activity. The current multi-stimuli responsive cotton fibers displayed high reversibility without fatigue. The morphology of AHPV nanoparticles was studied by TEM demonstrated to show diameters of 74–92 nm. The morphology properties of the AHPV-finished textiles were studied by SEM, EDX, and FTIR analyses. The mechanical and colorfastness performance was also reported for the chromogenic cotton fabrics. The current strategy can be reported as an easy and affordable nanocomposite spray-coating method onto cotton fabrics with high durability for a wide range of applications, such as functional clothing, anti-counterfeiting, packaging, as well as medical and healthcare textiles.

2. Experimental

2.1. Reagents and materials

Cotton samples were supplied from Misr-Helwan Spinning and Weaving Co., Egypt. The supplied cotton fabric was characterized with thickness of 0.40 mm, warp 36 yarn/cm, weft 30 yarn/cm, plain weave (150 g/m^2), micronaire (3.88 Âµg/inch)

and micronaire (3.88 Âµg/inch). The fabrics were scoured and bleached relying on previous procedure (Al-Qahtani et al., 2021). TLC (silica gel 60 F$_{254}$) was used to follow up the reaction progress. The generated compounds were purified by silica gel 60 through column chromatography. Both of dialdehyde **1** and dihydrazide **2** were synthesized depending on previous procedures (Ciepluch et al., 2012; Li et al., 2013). The resin binder was provided by Dystar (Egypt). The acetylene diol, mineral oil, and oleoresin were supplied from Fluka and Sigma-Aldrich (Egypt).

2.2. Preparation of AHPV

The acylhydrazone-based polyviologen (AHPV) was prepared using previous method (Al-Qahtani et al., 2022b) as shown in Scheme 1. The dihydrazide compound **1** was subjected to supramolecular condensation polymerization with the π-electron deficient dialdehyde bipyridinium compound **2** in aqueous medium (pH = 2–3). A solution of compound **1** (302.4 mg, 1.44 mmol) in a acetic acid/de-ionized water (1:5 mL) was added to a solution of compound **2** (804 mg, 1.44 mmol) in de-ionized water (20 mL). The provided mixture was stirred at 95 °C, and then left to settle for 24 hrs under ambient conditions. The produced mixture was decanted into a Petri dish, frozen in a refrigerator at –80 °C, and then freeze-dried at –50 °C (0.1 mbar) employing freeze-dryer equipment (Christ Alpha 1–2 LD Plus) to provide the solid-state acylhydrazone-based polyviologen xerogel as a yellow powder (78%); GPC (DMF): Mp, Mn, Mw, Mz, (Mz + 1), Mv, and polydispersing index were reported at 12,100 g mol^{-1}, 9,200 g mol^{-1}, 10,400 g mol^{-1}, 10,900 g mol^{-1}, 12,100 g mol^{-1}, 11,100 g mol^{-1}, and 1.08, respectively.

2.3. Preparation of multichromic textiles

A mixture of alkyd resin (25%; w/w), ammonium hydroxide (1% w/w), mineral oil (10%; w/w), oleoresin (50%; w/w), dry-ing agent (0.5%; w/w), and acylhydrazone-based polyviologen (AHPV) was stirred for 2 hrs to accomplish a consistent dispersion. The solution was homogenized (25 kHz) for 20 min, followed by the addition of acetylene diol (1%; w/w) with stirring. Different composites were developed using different ratios of AHPV, including 0, 0.1, 0.3, 0.6, 0.9, 1.2, 1.5, 1.8 and 2.1% w/v. The formulated composites were spray-coated onto cotton fabrics (15 × 15 cm) employing automatic spray gun (Lumina; STA6R; Fuso Seiki; Japan). The AHPV-finished cotton samples were air-dried, and represented by AHPV$_0$, AHPV$_1$, AHPV$_2$, AHPV$_3$, AHPV$_4$, AHPV$_5$, AHPV$_6$, AHPV$_7$, and AHPV$_8$, respectively. Fig. 1 shows a schematic diagram for the preparation steps of multichromic cotton fabrics.

2.4. Methods and devices

Bruker Avance (400 MHz) was employed at room temperature to record the NMR spectrum. The morphology and elemental content of the AHPV-finished cotton samples were examined using Quanta SEM FEG250 (Czech Republic) coupled to TEAM-EDX. The AHPV-finished cotton fabrics were annealed for 12 h at 45 °C, and then sputtered with gold film (10 nm) for SEM analysis. We measured the diameters of AHPV nanoparticles using a transmission electron microscope (TEM; JEOL 1230; Japan). A suspension of AHPV nanopowder in distilled water was homogenized for 5 min, and then dropped onto a Cu-grid for TEM analysis. Nicolet Nexus 670 FTIR spectroscopy (United States) was utilized to analyze the substituents on the AHPV-finished cotton surface. Gel Permeation Chromatography (GPC; Agilent PL-220; USA) was employed to study the AHPV nanoparticles in DMF. PANalytical Pro XPert XRD with CuK$_α$ was utilized to record the solid AHPV crystallographic structure. The thermal properties of the AHPV nanoparticles were studied by Perkin Elmer TGA STA6000. In order to evaluate the comfort properties of the AHPV-finished cotton fabrics, both of bend length
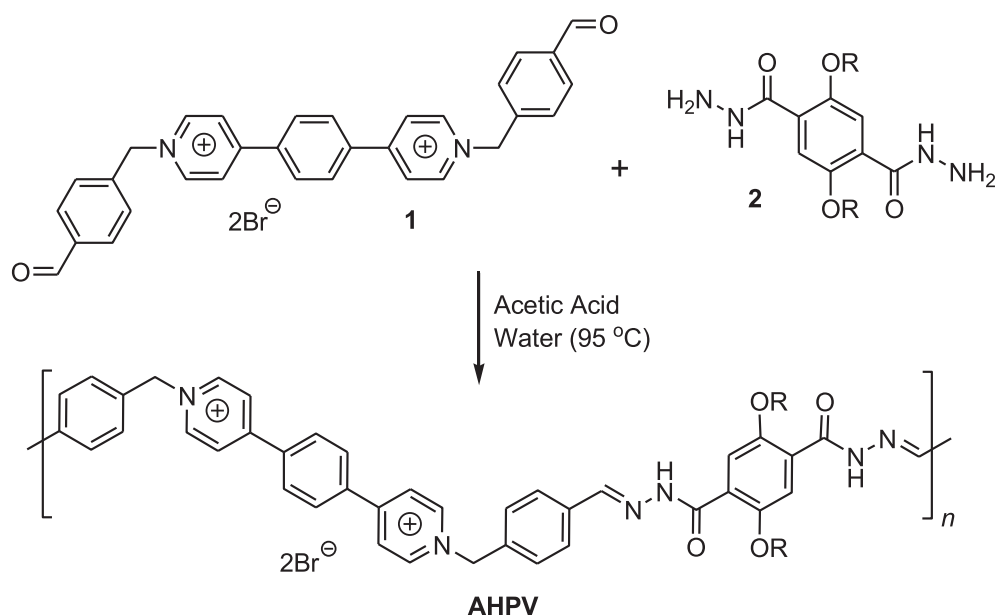
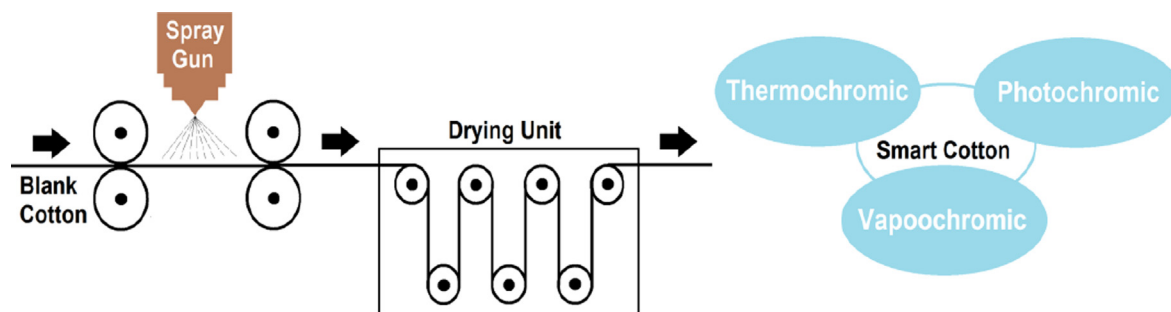**Scheme 1**   Preparation steps of AHPV; R = C$_3$H$_7$.

Fig. 1 Schematic diagram displaying the preparation steps of multichromic cotton fabrics.

and air-permeability were studied by Shirley Stiffness under the British 3356:(1961) standardized test, and Textest FX3300 under the ASTM D737 standard method, respectively.

2.5. Colorfastness and colorimetric properties

UltraScan Pro (HunterLab; United States) was utilized to report both CIE Lab and color strength (K/S) data of AHPV-finished fabrics before and after exposure to the chromic activity, including heat (thermochromic), UV light (photochromic), and ammonia (vapochromic). The CIE (International Commission on Illumination or known as Commission Internationale de L'éclairage) Lab parameters were used to describe colors as 3D numerical values; where L* describes colors from brightest white (100) to darkest black (0); a* describes colorimetric data from green (–a*) to red (+a*); and b* describes colorimetric data from blue (–b*) to yellow (+b*). The thermochromic behavior of the AHPV-finished fabric was monitored with raising the temperature (25–85 °C), while recording the absorbance spectra. The vapochromism was studied by exposure to gaseous ammonia liberated from a test tube full of NH_4OH_{aq}, while recording the absorbance spectra by using UltraScan Pro (HunterLab; United States). Similarly, the absorbance spectra of the AHPV-finished fabric were collected under visible and UV lights.

2.6. Reversibility and durability

For several cycles, the absorbance spectra of the AHPV-finished fabric were collected under air and gaseous ammonia (vapochromism), under visible and UV lights (photochromism), and under 25 °C and 85 °C (thermochromism). The colorfastness properties of the AHPV-finished fabrics were determined under ISO105 (B02:1988) for light, ISO105 (C02:1989) for washing, ISO105(X12:1987) for rubbing, and ISO105(E04:1989) for perspiration. Photographs demonstrating the photochromic, vapochromic and thermochromic behaviors of cotton fabrics were taken by Canon A710IS.

2.7. Cytotoxicity assay

The *in vitro* cytotoxicity of the AHPV$_8$-finished fabric with the highest concentration of AHPV was examined under MTT proliferation (Sigma-Aldrich) utilizing epithelial cell lines

(Al-Qahtani et al., 2022a). The cytotoxicity (%) was reported by equation (1).

$$Cytotoxicity\% = \left[\frac{Reading\ of\ sample}{Reading\ of\ negative\ control} - 1 \right]$$
$$\times\ 100 \tag{1}$$

3. Result and discussion

3.1. Morphological properties

The acylhydrazone-based polyviologen (AHPV) was prepared by polycondensation of bipyridinium dialdehyde **1** with dihydrazide **2** in an acidic de-ionized water. ^{1}H NMR spectrum of AHPV was difficult to analyze owing to its poor solubility in deuterated solvents. Broad peaks were monitored by carrying out the polycondensation in deuterated water (D_2O), and in the presence of a deuterated acetic acid (aceticacid d_4). ^{1}H NMR spectrum demonstrated peaks for O–H and N–H at 10.36 and 12.06 ppm, respectively. The phenyl protons were detected as multiplet signal at 7.89–7.49 ppm. The viologen protons, (N = C–H) and (C = C–H), were detected at 9.45 and 8.70 ppm, respectively. A broad signal was monitored at 5.98 ppm due to the methylene (CH_2) protons. Both of polydispersity index and molecular weight of the acylhydrazone-based polyviologen were reported by GPC in DMF to indicate an average molecular weight. Fig. 2 shows TEM images of acylhydrazone-based polyviologen (AHPV) nanoparticles, demonstrating average diameters of 74–92 nm. This miniaturized particle size of the acylhydrazone-based polyviologen nanoparticles helped to create an even distribution of AHPV nanoparticles onto the finished fabrics.

Fig. 3 illustrates the XRD analysis of the acylhydrazone-based polyviologen nanoparticles' crystallinity. A d-spacing allowed us to monitored wide bands at $2\theta = 6.89, 14.77$ and $34.51°$. Thus, multiple π-stacking attraction forces were included inside the substance; but the material was mostly amorphous (Al-Qahtani et al., 2022b). Sharp peak was detected at $2\theta = 22.76°$, which could be reported as signatures of ion-paired bromide counter ions (Ma et al., 2020; Al-Qahtani et al., 2022b).

Improved dispersion of the AHPV-encapsulated cross-linked resin film onto the finished cotton fabric surface was achieved by using acylhydrazone-based polyviologen in the nanoparticle form. The multichromic nanocomposite was applied onto cellulose cotton fabrics by spray-coating. Spray-
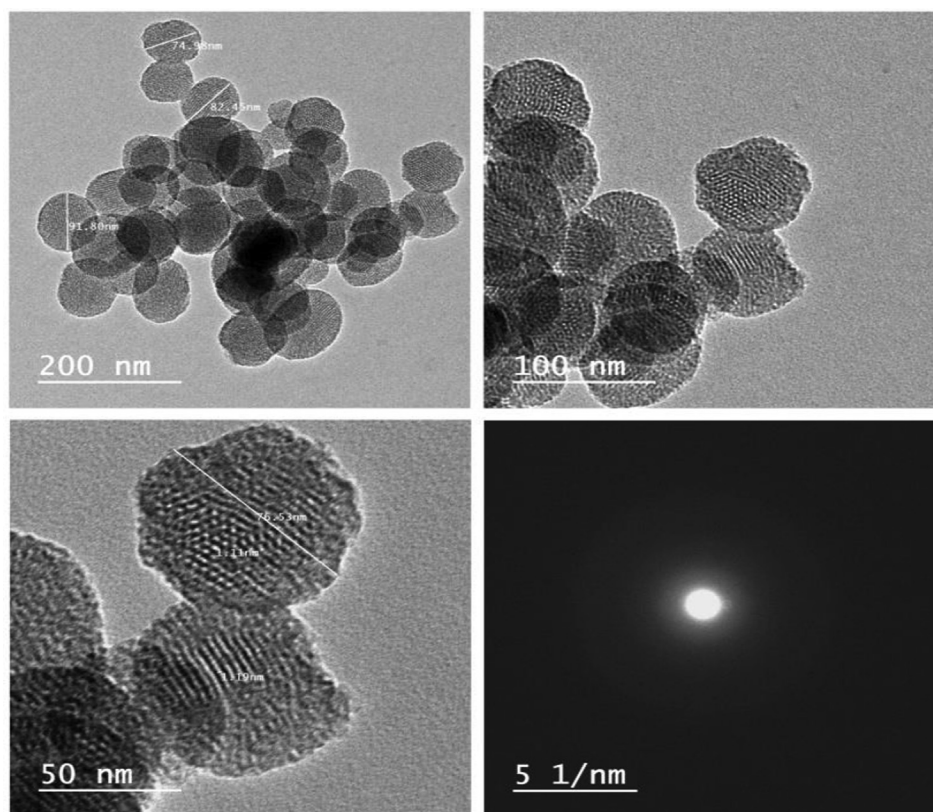
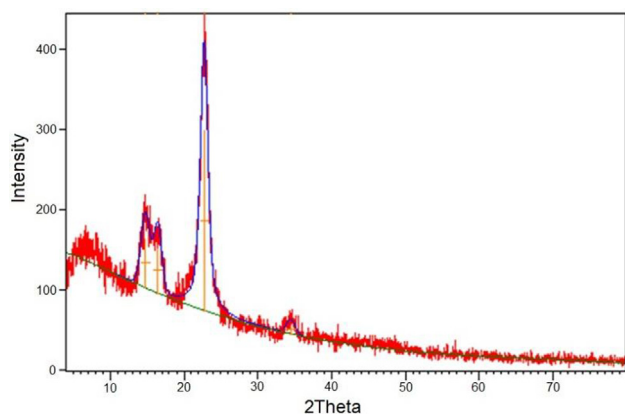**Fig. 2** TEM images of acylhydrazone-based polyviologen nanoparticles.

Fig. 3 X-ray diffraction of acylhydrazone-based polyviologen nanopowder.

coating technology has been characterized by high deposition efficiency and rate, low cost, and maintaining flexibility, permeability and appearance of the coated substrate (Samanta and Bordes, 2020). It is shown in Fig. 4 that the surface morphology of the AHPV-finished cotton fabrics was investigated by SEM microscopy. The micrographs taken with a scanning electron microscope showed that the AHPV nanoparticles were successfully deposited onto the fabric surface as compared to blank cotton (Zhang et al., 2021). The AHPV nanoparticles were successfully dispersed throughout the finished cotton fabrics by the spray-coating technology. The

excellent dispersion of the AHPV nanoparticles onto cotton surface could be explained by the development of hydrogen bonding between the AHPV polymer chains and the cellulosic hydroxyl groups (Al-Qahtani et al., 2022b). Despite the dispersion of the composite particles onto the fabrics surface, the cotton surface displayed the same fibrous morphology as blank cotton without deformation. The AHPV distribution in resin film immobilized into cotton surface was shown to be uniform by EDS (Table 1). Bromine and nitrogen were found to be minor compositions due to AHPV in comparison to carbon and oxygen which are major compositions in the cellulosic cotton fabric and resin binder.

Both homogeneous coating and elemental contents of the AHPV-finished cottons were studied by EDAX. The distribution of AHPV nanoparticles onto AHPV-finished cottons was found to be uniform, since the elemental contents were almost identical at the three scanned sites on the sample surface. The EDAX analysis was found to match with the molar ratios of elements utilized in the preparation of AHPV and finished fabrics. In order to study the chemical functional groups on cotton surface, the FT-IR technique has proven a key analytical tool. Thus, FTIR spectroscopy could be utilized to determine the mechanism of the chromic composite's attachment onto the cellulose cotton fabric. Fig. 5 shows the FT-IR spectroscopic data for $AHPV_0$, $AHPV_1$, and $AHPV_8$. The hydroxyl substituents on blank cotton cellulose were identified by the absorbance intensity at 3431 cm^{-1}. To validate the existence of the glucose aliphatic units, the absorption at 2924 cm^{-1} was detected (El-Newehy et al., 2021). Cellulosic cellulose and resin bond strongly once the nanoparticles of AHPV are
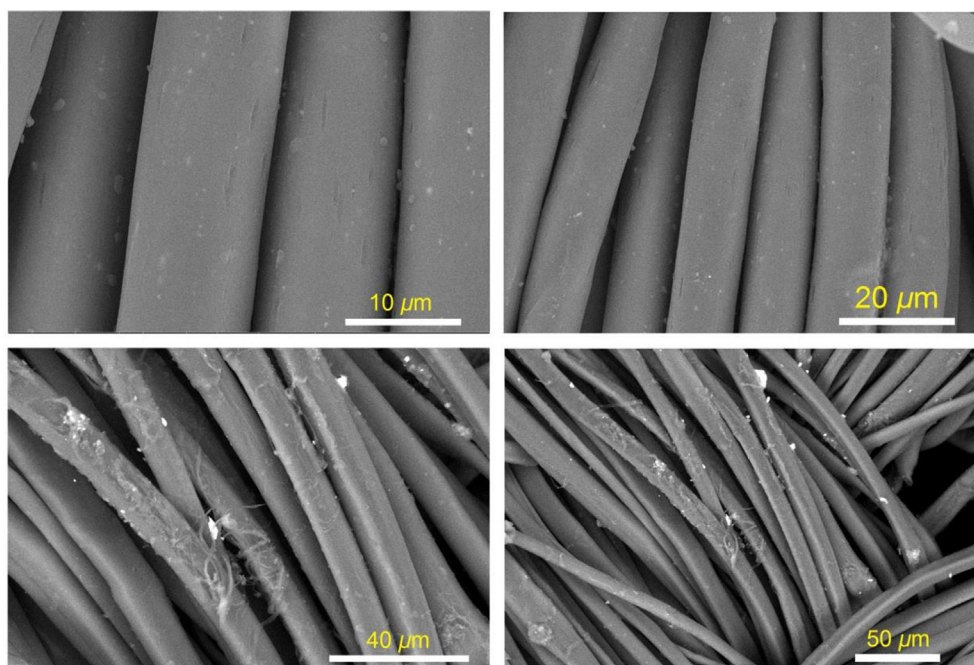
Fig. 4 SEM images of AHPV$_1$ (a-c), and AHPV$_8$ (d-f).

Table 1 Chemical compositions of AHPV$_0$, AHPV$_1$, AHPV$_6$, and AHPV$_8$ at three scanned points (a$_1$, a$_2$ and a$_3$) on cotton surface.

Fabric		C	O	Br	N
AHPV$_0$		66.17	33.83	0	0
AHPV$_1$	a$_1$	66.84	33.54	0.27	0.35
	a$_2$	66.90	33.64	0.25	0.41
	a$_3$	66.78	33.37	0.35	0.50
AHPV$_6$	a$_1$	65.54	33.04	1.15	1.23
	a$_2$	65.40	33.16	1.13	1.31
	a$_3$	65.37	33.18	1.24	1.21
AHPV$_8$	a$_1$	65.00	32.87	1.44	1.65
	a$_2$	65.14	32.72	1.44	1.70
	a$_3$	65.03	32.78	1.55	1.64

Fig. 5 FTIR spectra of AHPV-finished cotton fabrics; AHPV$_0$ (a), AHPV$_1$ (b), and AHPV$_8$ (c).

embedded in the transparent layer (Al-Qahtani et al., 2022b). The resin carbonyl ester displayed an absorption band at 1709 cm^{-1}. The hydroxyl absorbance peaks were found to shift from 3431 cm^{-1} for blank cotton to 3357 cm^{-1} for the finished cotton fabrics. Likewise, the absorbance band of the resin carbonyl ester was observed to shift from 1709 cm^{-1} for blank cotton fabric to 1610 cm^{-1} for the finished cotton fabrics (Ghasemzadeh et al., 2022). Furthermore, decreases in the absorbance peaks of cellulosic hydroxyl and resin carboxyl groups were detected after spray-coating. This could be ascribed to the formation of H-bonds between alkyd resin hydroxyl groups and hydroxyl groups on cotton cellulose polymer chains (Al-Qahtani et al., 2022b). Similarly, the absorption intensity of these hydroxyls decreased when the AHPV ratio was increased.

TGA was used to better understand AHPV nanoparticles's thermal stability, which is significant during the exploration of the thermochromic activity. When heated to 285 °C, the AHPV nanopowder showed thermal stability with two major
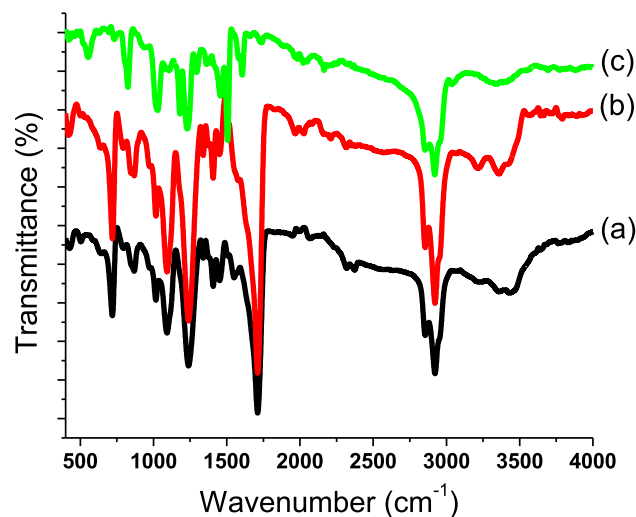
stages of thermal properties, suggesting three distinct thermal states. Temperatures in the first phase ranged from 25 °C to 190 °C due to evaporation of moisture. In the second phase, temperatures ranged from 190 °C to 340 °C, demonstrating ∼ 45% loss of weight due to thermal decomposition of AHPV.

3.2. Vapochromism of cotton

Materials that can alter their physical characteristics, like color, responding to one or more external stimuli are referred to as "smart products". Photochromic, thermochromic and vapochromic materials can alter their colors when exposed

to one or more external stimuli, including light, heat and vapor, respectively. Chromic materials can be used as early warning devices for security alerts, sensors and anticounterfeiting applications, which have lately received more attention. The development of colorimetric sensors capable of detecting both gaseous and aqueous ammonia has proven to be a difficult challenge. Ammonia as a Lewis base, while the bipyridinium part of AHPV functions has been reported as a Lewis acid (Skorjanc et al., 2019). This induced the transfer of electrons from ammonia to bipyridinium, inducing the color switch from pale yellow to green by forming a bipyridinium radical-cation. Microfibrous cellulosic fabric has a large surface area, allowing easy adsorption of ammonia molecules onto cotton surface and diffusion through the mesh to offer excellent detection sensitivity (Bahari et al., 2020; Blundo et al., 2021; Li et al., 2021). The color of the gaseous ammonia rapidly changed from pale yellow to green in less than a second of exposure. Strong absorption band appeared at 593 nm was shown to be correlated to this color change (Figs. 6-7). When the ammonia gas source was shielded from the sprayed cotton sample, the color quickly returned to pale yellow at 437 nm. When the ammonia exposure/shielding procedure was repeated numerous times, the results in Fig. 8 showed good reversibility and fatigue resistance. The current ammonia detection tool can be applied for various fields, including human and environmental protection, as well as foodstuffs quality control.
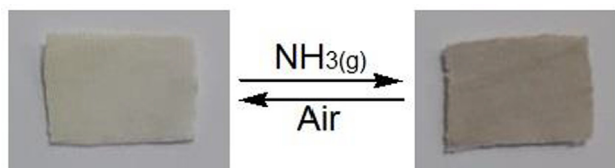

Fig. 6 Photographs showing reversible color change under atmospheric and $NH_{3(g)}$.

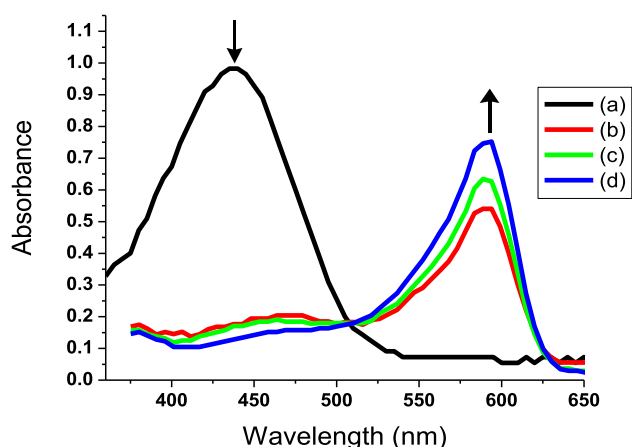**Fig. 7** Absorbance spectra of cotton fabric immobilized with acylhydrazone-based polyviologen ($AHPV_6$) using different $NH_{3(aq)}$ concentrations; 0 (a), 50 (b), 100 (c), and 150 (d) ppm. Increasing the aqueous ammonia concentration demonstrated a considerable effect on both absorption wavelength and intensity of the chromogenic fabric.
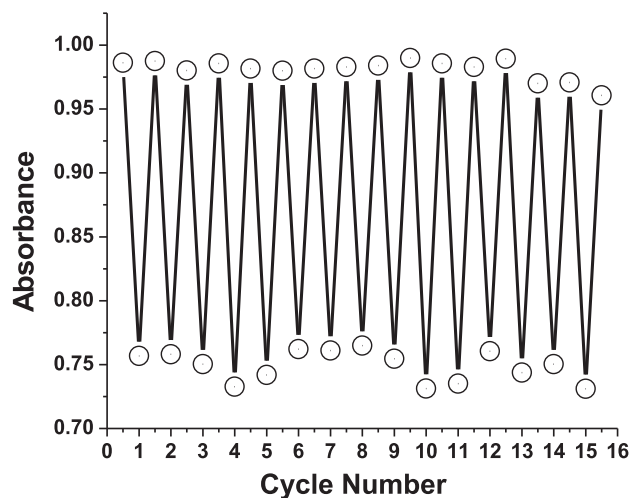

Fig. 8 Variations in absorption intensity of $AHPV_6$ at 437 and 593 nm demonstrating a reversible colorimetric change under gaseous ammonia (green) and atmospheric (pale yellow) conditions.

Using colorimetric screening under exposure to atmospheric and gaseous ammonia, the AHPV-finished cottons were evaluated upon varying the concentration of acylhydrazone-based polyviologen as shown in Table 2. It was noticeable that the AHPV-finished cotton textiles had a pale yellow color. When the AHPV ratio was increased under atmospheric conditions, the K/S ratio remained almost unchanged. When exposed to ammonia gas and increasing the AHPV ratio from $AHPV_1$ to $AHPV_6$, the K/S value was found to significantly increase. With the further increase of the AHPV ratio from $AHPV_6$ to $AHPV_8$, there was a modest rise in K/S in the presence of ammonia gas, suggesting that the $AHPV_6$ cotton sample had the best colorimetric data. Exposure to ammonia gas caused the absorbance wavelength to shift from 437 nm to 593 nm (Bathochromic shift), which resulted in a dramatic change in color. When the AHPV ratio was increased under atmospheric conditions, the effect on L* was minimal. A colorimetric switch from yellow to green was monitored following exposure to ammonia, which results in a considerable decrease in L*. Both a* and b* of the AHPV-finished cotton textiles showed positive values under atmospheric conditions, indicating a pale yellow color. The + a* values change to –a* after exposure to ammonia gas, indicating a color shift from pale yellow to green.

The chromogenic fabric ($AHPV_6$) was immersed for 5 s in different concentrations of NH_4OH_{aq} to measure the LOD of $NH_{3(aq)}$. After air-drying, the colorimetric changes in absorption intensity of the $AHPV_6$-finished cotton fabric was explored. The absorption intensity rose from 437 to 593 nm when the ammonia content increased from 50 to 150 ppm, as depicted in Fig. 7. The absorbance peak at 593 nm was firstly appeared at an ammonia concentration of 50 ppm. The absorption intensity (593 nm) increases as the $NH_{3(aq)}$ concentration increases. For ammonia concentrations more than 150 ppm; however, no additional increases in absorbance intensity were observed. Thus, the detection limit was monitored between 50 and 150 ppm for $NH_{3(aq)}$.

Table 2 Colorimetric screening chromogenic fabrics at various ratios of acylhydrazone-based polyviologen under air and NH$_{3aq}$.

AHPV Conc.	L*		a*		b*		K/S	
	air	NH$_{3aq}$	air	NH$_{3aq}$	air	NH$_{3aq}$	air	NH$_{3aq}$
Blank	94.35	94.78	0.06	0.10	1.18	1.30	0.13	0.17
AHPV$_1$	86.83	67.49	2.05	−12.17	20.58	16.01	0.32	2.14
AHPV$_2$	85.19	66.32	3.14	−13.51	18.27	15.37	0.51	2.61
AHPV$_3$	84.52	65.74	5.34	−15.72	15.65	13.19	0.81	3.38
AHPV$_4$	84.28	64.63	8.91	−18.47	12.94	9.32	1.06	4.58
AHPV$_5$	81.05	63.11	11.07	−26.06	9.88	6.01	1.19	5.12
AHPV$_6$	80.02	61.60	12.29	−27.15	7.84	4.87	1.39	6.13
AHPV$_7$	79.29	60.04	12.78	−29.30	7.07	3.84	1.61	6.87
AHPV$_8$	78.33	59.25	13.92	−34.69	5.99	3.27	1.83	8.09

3.3. Thermochromic activity of AHPV-coated cotton

To produce the green radical cation, the charge transfer between the AHPV bipyridinium dication part and its counter anion could be activated by heating (Skorjanc et al., 2019; Bahari et al., 2020; Blundo et al., 2021; Li et al., 2021). The thermochromic properties of the AHPV-finished cotton are shown in Fig. 9. Both of CIE Lab and absorbance spectra were used to illustrate thermochromic activity to green of the yellow colored AHPV$_6$ as shown in Table 3. Considerable differences
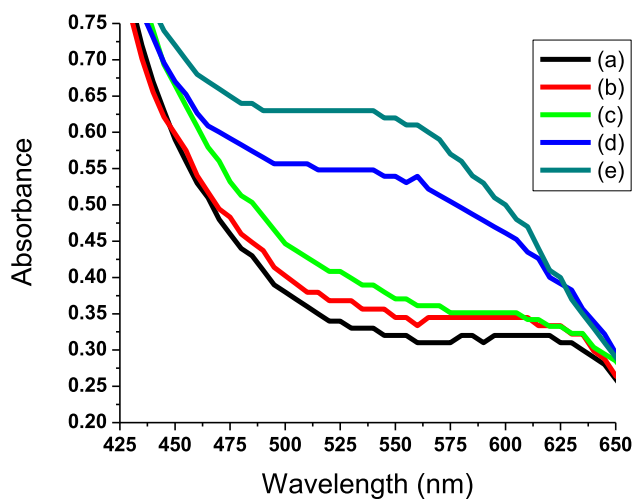
in CIE Lab and K/S were monitored when temperatures were raised from 25 to 85 °C, suggesting the development of a green color. L* decreased when the temperature was raised to demonstrate a color shift from pale yellow to green. The thermal stability and durability of the AHPV-finished cotton was studied by exposure to alternative heating/cooling cycles to designate high reversibility and durability (Fig. 10). Both a* and b* of AHPV$_6$ showed positive values at room temperature, indicating a pale yellow color. The + a* value changed to –a* with raising the temperature from 25 °C to 85 °C, indicating a colorimetric shift to green. However, no considerable changes in either the absorption wavelength or intensity were detected with increasing the temperature from 25 to 35 °C as the initial changes in the colorimetric properties were detected at 45 °C. Additionally, the absorption wavelength was detected

Fig. 9 Absorption spectra of AHPV$_6$ at 45 (a), 55 (b), 65 (c), 75 (d), and 85 (e) °C.
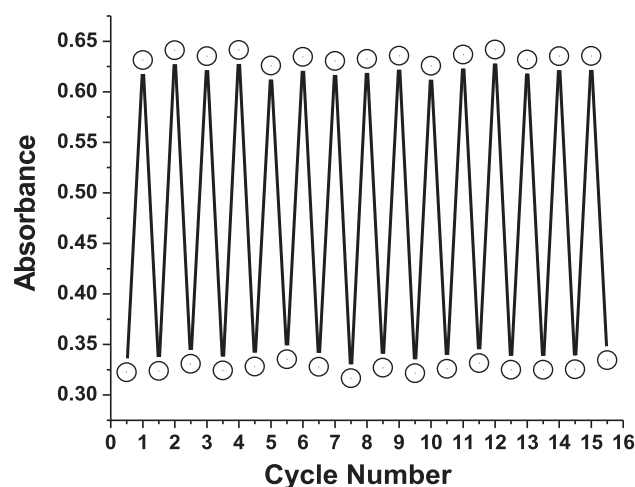
Fig. 10 Absorbance intensity of AHPV$_6$ at 607 nm (45 °C) and 514 nm (85 °C).

Table 3 Color screening of AHPV$_6$ as a function of temperature.

Temp. (°C)	L*	a*	b*	K/S
25	80.02	12.29	7.84	1.39
35	80.07	12.37	7.43	1.51
45	76.35	−15.08	4.81	2.67
55	71.34	−17.01	4.34	2.93
65	67.00	−19.10	3.92	3.41
75	63.54	−23.29	3.28	4.29
85	60.87	−26.47	2.71	4.85

Table 4 Colorimetric screening of AHPV$_6$ as a function of temperature.

Condition	L*	a*	b*	K/S
Visible	80.02	12.29	7.84	1.39
Ultraviolet	67.24	−18.02	3.81	3.06

Fig. 11 Normalized absorbance spectra of AHPV$_6$ underneath visible (b), and ultraviolet lights (b).

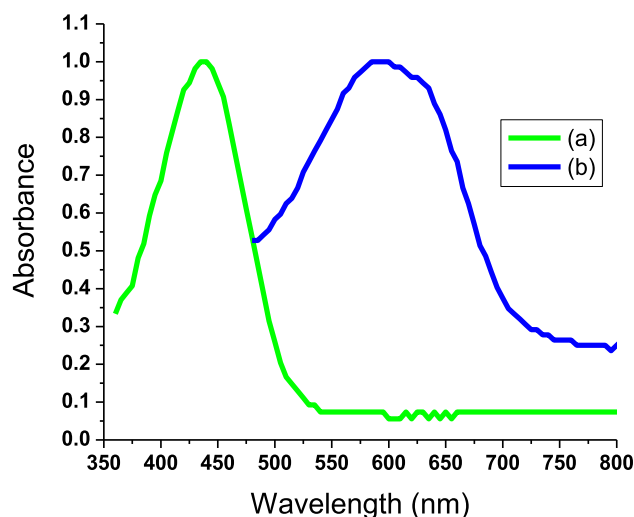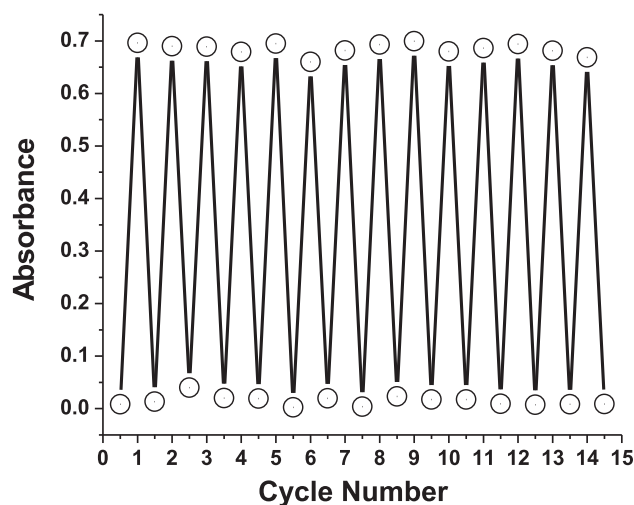**Fig. 12** Absorbance intensity of AHPV$_6$ at 593 nm under visible and ultraviolet lights.

to shift from 607 nm to 514 nm with increasing the temperature from 45 to 85 °C, respectively. Similarly, the absorption intensity was detected to increase with increasing the temperature from 45 to 85 °C.

3.4. Photochromism of AHPV-finished cotton

The color change of the pale yellow spray-coated fabrics to green under UV irradiation was studied using CIE Lab and K/S screening as illustrated in Table 4. In the absence of acylhydrazone-based polyviologen, AHPV$_0$ exhibited the same light yellow color as compared to the AHPV-finished cottons (AHPV$_1$ – AHPV$_8$). Increasing the AHPV concentration from AHPV$_1$ to AHPV$_8$ resulted in a little deeper yellow color under daytime light. With increasing AHPV concentration, the CIE Lab and K/S displayed significant shifts under UV as compared to those under daytime light that indicated deeper green color. The L* value decreased, suggesting that the color had changed from light yellow to green as a result of UV irradiation. Both a* and b* of AHPV$_6$ showed positive values under daytime light to indicate a pale yellow color. However, the + a* shifted to –a* under UV light to designate a color switch to green.

The maximum absorption wavelength demonstrated a bathochromic shift to a longer wavelength from 437 nm to 593 nm upon exposure to ultraviolet light. All AHPV-finished cotton fabrics showed reversible photochromism with the same absorption wavelength at 593 nm (Fig. 11). All sprayed yellow fabrics displayed rapid and reversible photochromic green color upon irradiation with UV light. This green color was reversed upon removing the ultraviolet supply.

The bipyridinium dication electron-deficiency produces radical cations due to photocatalyzed transfer of electrons from the counter anions to the AHPV bipyridinium part. Generally, the green color arises due to intramolecular charge transfer among positively charged nitrogen (+) and neutral nitrogen. Moreover, the absorbance intensity at 593 nm was monitored to increase with raising the irradiation interval time owing to accumulation of radical cations intensity (Skorjanc et al., 2019; Bahari et al., 2020; Blundo et al., 2021; Li et al., 2021). In order to evaluate the fatigue resistance to ultraviolet light, the absorbance spectra of AHPV-finished fabric were collected under visible and UV lights for several cycles to indicate high photostability as shown in Fig. 12.

Table 5 Colorfastness of spray-coated fabrics.

AHPVConc.	Washing		Perspiration				Crocking		Sublimation		Light
	Alt*	St**	acid		Base		Dry	Wet	180 °C	210 °C	
			Alt	St	Alt	St					
AHPV$_1$	4–5	4–5	4–5	4–5	4–5	4–5	4–5	4–5	4–5	4–5	6–7
AHPV$_2$	4–5	4–5	4–5	4–5	4–5	4–5	4–5	4–5	4–5	4–5	6–7
AHPV$_3$	4–5	4–5	4	4–5	4–5	4–5	4–5	4–5	4–5	4–5	6–7
AHPV$_4$	4	4	4	4–5	4–5	4–5	4–5	4–5	4–5	4	6–7
AHPV$_5$	4	4–5	4	4–5	4	4–5	4–5	4	4–5	4	6
AHPV$_6$	4	4	4	4	4	4–5	4–5	4	4–5	4	6
AHPV$_7$	4	4	3–4	4	4	4	4	3–4	4–5	4	6
AHPV$_8$	3–4	3–4	3–4	3–4	3–4	4	3–4	3–4	3–4	3	5–6

* Alt describes alteration of fabric color; **St describes staining to cotton.

Table 6 Effect of AHPV concentration of bending length (BL) and air-permeability (AP) of spray-coated fabrics.

AHPV Conc.	BL (cm)		PA ($cm^3/cm^2.s$)
	weft	*wrap*	
Blank	2.60 ± 1.2	2.97 ± 1.0	52.82 ± 1.4
$AHPV_1$	2.95 ± 1.2	3.15 ± 1.7	52.14 ± 1.0
$AHPV_2$	3.01 ± 1.0	3.23 ± 1.3	51.95 ± 1.1
$AHPV_3$	3.12 ± 1.3	3.34 ± 1.1	51.73 ± 1.2
$AHPV_4$	3.24 ± 1.3	3.41 ± 1.2	51.57 ± 1.0
$AHPV_5$	3.35 ± 1.1	3.50 ± 1.1	51.30 ± 1.1
$AHPV_6$	3.42 ± 1.5	3.60 ± 1.0	51.02 ± 1.3
$AHPV_7$	3.56 ± 1.4	3.75 ± 1.2	50.87 ± 1.4
$AHPV_8$	3.84 ± 1.0	3.90 ± 1.1	50.75 ± 1.2

Table 7 Cytotoxic screening of AHPV-finished cotton fabrics at 100 ppm.

Notes	IC_{50} (ppm)	IC_{90} (ppm)	Fabric
0	–	–	$AHPV_0$
0	–	–	$AHPV_1$
0	–	–	$AHPV_3$
0	–	–	$AHPV_6$
0	–	–	$AHPV_8$
0	–	–	Negative control
0	–	–	DMSO

3.5. Durability and comfort characteristics

Excellent softness to touch was detected for the cotton textiles finished with the acylhydrazone-based polyviologen. Both of tinctorial strength and colorfastness of AHPV-finished cotton fabrics demonstrated good to excellent results as shown in Table 5. Good colorfastness to sublimation was monitored, and no considerable discriminations were observed among the heat-press temperatures at 180 °C and 210 °C. However, the poorest colorfastness was detected when using higher concentrations of the acylhydrazone-based polyviologen; $AHPV_7$ and $AHPV_8$. In order to assess the physico-mechanical and comfort properties of the spray-coated cottons, both air-permeability and flexibility were reported as shown in Table 6. The AHPV-finished fabrics showed almost no negative impacts on their air-permeability; however, a slight decrease in fabric flexibility was monitored with increasing the concentration of the acylhydrazone-based polyviologen.

3.6. Cytotoxicity screening

The MTT test was used to measure the cytotoxic activity (*in vitro*) because the present diagnostic cotton assay could be used in different clinical and foodstuff packaging purposes (Al-Qahtani et al., 2022a). As shown in Table 7, no cytotoxicity was observed even for the cotton biosensor with the highest concentration of acylhydrazone-based polyviologen.

4. Conclusion

Smart cotton textiles having thermochromic, photochromic and vapochromic characteristics, as well as high reversibility without fatigue, were developed. The acylhydrazone-based polyviologen (AHPV) copolymer was synthesized by simple and eco-friendly supramolecular polycondensation in an acidified aqueous medium. To develop efficient multi-stimuli responsive composite films for protective textiles, AHPV was deposited onto cotton fabrics without significantly impacting the treated cotton fabrics' mechanical and physical characteristics. AHPV was deposited by the spray-coating technology onto cotton fabrics using alkyd resin as a trapping binder. Colorimetric shifts from pale yellow to green were observed on the produced textiles as a result of increasing temperature (thermochromic) from room temperature to 85 °C. Similarly, exposure to ammonia gas (vapochromic) and UV light (photochromic) triggered the color change of the chromogenic textiles. The AHPV-finished cotton textiles were soaked in different concentrations of aqueous ammonia to indicate a limit of detection in the range of 50–150 ppm. The spray-coated cotton fabrics exhibited two absorbance peaks at 437 nm (pale yellow) and 593 nm (green) under vapochromic and photochromic activities, while two absorbance peaks were detected at 607 nm (45 °C) and 514 nm (85 °C) under thermochromic activity. By using TEM, the morphology of AHPV nanoparticles demonstrated diameters of 74–92 nm. There were no noticeable variations in the fibrous structure of the AHPV-finished cotton textiles as compared to the blank fabric, as shown by SEM, EDX, and FTIR analyses. CIE Lab and absorption spectra proved the ultraviolet-, temperature-, and ammonia-dependent colorimetric shifts from pale yellow to green. The physico-mechanical characteristics of the spray-coated samples differed slightly from those of the blank cotton. Good to excellent colorfastness performance was reported for the chromogenic fabrics. An easy and affordable composite coating with great durability was developed and spray-coated onto cotton fabrics for a wide range of applications, such as functional clothing, anticounterfeiting, medical and packaging textiles.

Declaration of Competing Interest

The authors declare that they have no known competing financial interests or personal relationships that could have appeared to influence the work reported in this paper.

References

Aburas, M., Soebarto, V., Williamson, T., Liang, R., Ebendorff-Heidepriem, H., Wu, Y., 2019. Thermochromic smart window

technologies for building application: A review. Appl. Energy 255, 113522.

Al-Qahtani, S.D., Alzahrani, H.K., Azher, O.A., Owidah, Z.O., Abualnaja, M., Habeebullah, T.M., El-Metwaly, N.M., 2021. Immobilization of anthocyanin-based red-cabbage extract onto cellulose fibers toward environmentally friendly biochromic diagnostic biosensor for recognition of urea. J. Environ. Chem. Eng. 9, (4) 105493.

Al-Qahtani, S.D., Snari, R.M., Al-Ahmed, Z.A., Hossan, A., Munshi, A.M., Alfi, A.A., El-Metwaly, N.M., 2022a. Novel halochromic hydrazonal chromophore immobilized into rice-straw based cellulose aerogel for vapochromic detection of ammonia. J. Mol. Liq. 350, 118539.

Al-Qahtani, S.D., Snari, R.M., Alamrani, N.A., Aljuhani, E., Bayazeed, A., Aldawsari, A.M., El-Metwaly, N.M., 2022b. Synthesis and adsorption properties of fibrous-like aerogel from acylhydrazone polyviologen: efficient removal of reactive dyes from wastewater. J. Mater. Res. Technol. 18, 1822–1833.

Atav, R., Ergünay, U., Akkuş, E., 2022. Producing garment based multichromic smart sensors through dyeing cotton fabrics with chromic dyes. Cellulose 29 (1), 571–604.

Bahari, M., Malmberg, M.A., Brown, D.M., Nazari, S.H., Lewis, R.S., Watt, G.D., Harb, J.N., 2020. Oxidation efficiency of glucose using viologen mediators for glucose fuel cell applications with non-precious anodes. Appl. Energy 261, 114382.

Blundo, E., Polimeni, A., Meggiolaro, D., D'Annibale, A., Romagnoli, L., Felici, M., Latini, A., 2021. Brightly Luminescent and Moisture Tolerant Phenyl Viologen Lead Iodide Perovskites for Light Emission Applications. J. Phys. Chem. Lett. 12 (23), 5456–5462.

Chen, G., Li, Y., Bick, M., Chen, J., 2020. Smart textiles for electricity generation. Chem. Rev. 120 (8), 3668–3720.

Cheng, Y., Zhang, X., Fang, C., Chen, J., Wang, Z., 2018. Discoloration mechanism, structures and recent applications of thermochromic materials via different methods: A review. J. Mater. Sci. Technol. 34 (12), 2225–2234.

Ciepluch, K., Katir, N., El Kadib, A., Felczak, A., Zawadzka, K., Weber, M., Klajnert, B., Lisowska, K., Caminade, A.M., Bousmina, M., Bryszewska, M., 2012. Biological properties of new viologen-phosphorus dendrimers. Mol. Pharm. 9 (3), 448–457.

Dan, Y., Popowski, Y., Buzhor, M., Menashe, E., Rachmani, O., Amir, E., 2020. Covalent surface modification of cellulose-based textiles for oil–water separation applications. Ind. Eng. Chem. Res. 59 (13), 5456–5465.

Ding, J., Zheng, C., Wang, L., Lu, C., Zhang, B., Chen, Y., Li, M., Zhai, G., Zhuang, X., 2019. Viologen-inspired functional materials: synthetic strategies and applications. J. Mater. Chem. A 7 (41), 23337–23360.

Eid, B.M., Ibrahim, N.A., 2021. Recent developments in sustainable finishing of cellulosic textiles employing biotechnology. J. Clean. Prod. 284, 124701.

El-Newehy, M.H., El-Hamshary, H., Salem, W.M., 2021. Solution blowing spinning technology towards green development of urea sensor nanofibers immobilized with hydrazone probe. Polymers 13 (4), 531.

Fabiani, C., Pisello, A.L., Bou-Zeid, E., Yang, J., Cotana, F., 2019. Adaptive measures for mitigating urban heat islands: The potential of thermochromic materials to control roofing energy balance. Appl. Energy 247, 155–170.

Fabiani, C., Castaldo, V.L., Pisello, A.L., 2020. Thermochromic materials for indoor thermal comfort improvement: Finite difference modeling and validation in a real case-study building. Appl. Energy 262, 114147.

Fan, J., Bao, B., Wang, Z., Xu, R., Wang, W., Yu, D., 2020. High tristimulus response photochromic cotton fabrics based on spiropyran dye by thiol-ene click chemistry. Cellulose 27 (1), 493–510.

Ghasemzadeh, B., Matin, A.A., Habibi, B., Ebadi, M., 2022. Cotton/Fe3O4@ SiO2@ H3PW12O40 a magnetic heterogeneous catalyst for biodiesel production: Process optimization through response surface methodology. Ind. Crops Prod. 181, 114806.

Gong, X., Hou, C., Zhang, Q., Li, Y., Wang, H., 2020. Thermochromic hydrogel-functionalized textiles for synchronous visual monitoring of on-demand in vitro drug release. ACS Appl. Mater. Interfaces 12 (46), 51225–51235.

Hakami, A., Srinivasan, S.S., Biswas, P.K., Krishnegowda, A., Wallen, S.L., Stefanakos, E.K., 2022. Review on thermochromic materials: development, characterization, and applications. J. Coat. Technol. Res., 1–26

Li, J., Guo, Y., Yao, H., Lin, Q., Xie, Y., Wei, T., Zhang, Y., 2013. A highly selective colorimetric sensor for Cu2 + based on phenolic group biscarbonyl hydrazone. Chin. J. Chem . 31 (2), 271–276.

Li, Z.H., Xue, L.P., Mu, Y.J., Zhao, B.T., 2021. Viologen-derived material showing photochromic, visually oxygen responsive, and photomodulated luminescence behaviors. CrystEngComm 23 (4), 1019–1024.

Libanori, A., Chen, G., Zhao, X., Zhou, Y., Chen, J., 2022. Smart textiles for personalized healthcare. Nat. Electron. 5 (3), 142–156.

Ma, T., Liu, L., Wang, J., Lu, Y., Chen, J., 2020. Charge storage mechanism and structural evolution of viologen crystals as the cathode of lithium batteries. Angew. Chem. Int. Ed. 59 (28), 11533–11539.

Oliveira, J., Correia, V., Castro, H., Martins, P., Lanceros-Mendez, S., 2018. Polymer-based smart materials by printing technologies: Improving application and integration. Addit. Manuf. 21, 269–283.

Persson, N.K., Martinez, J.G., Zhong, Y., Maziz, A., Jager, E.W., 2018. Actuating textiles: next generation of smart textiles. Adv. Mater. Technol. 3 (10), 1700397.

Ramlow, H., Andrade, K.L., Immich, A.P.S., 2021. Smart textiles: An overview of recent progress on chromic textiles. J. Text. Ins. 112 (1), 152–171.

Sadoh, A., Hossain, S., Ravindra, N.M., 2021. Thermochromic Polymeric Films for Applications in Active Intelligent Packaging—An Overview. Micromachines 12 (10), 1193.

Samanta, A., Bordes, R., 2020. Conductive textiles prepared by spray coating of water-based graphene dispersions. RSC Adv. 10 (4), 2396–2403.

Skorjanc, T., Shetty, D., Olson, M.A., Trabolsi, A., 2019. Design strategies and redox-dependent applications of insoluble viologen-based covalent organic polymers. ACS Appl. Mater. Interfaces 11 (7), 6705–6716.

Sun, K., Riedel, C.A., Urbani, A., Simeoni, M., Mengali, S., Zalkovskij, M., Bilenberg, B., De Groot, C.H., Muskens, O.L., 2018. VO2 thermochromic metamaterial-based smart optical solar reflector. ACS Photonics 5 (6), 2280–2286.

Wang, Q., Sun, J., Yao, Q., Ji, C., Liu, J., Zhu, Q., 2018. 3D printing with cellulose materials. Cellulose 25 (8), 4275–4301.

Xu, Y., Huang, L., Long, J., Zhang, R., Zhong, Z., Yang, L., Liu, L., Huang, Y., 2022. Reversible thermochromic POSS-Metal Films for early warning. Compos. Sci. Technol. 217, 109083.

Yang, W., Feng, Y., Si, Q., Yan, Q., Long, P., Dong, L., Fu, L., Feng, W., 2019. Efficient cycling utilization of solar-thermal energy for thermochromic displays with controllable heat output. J. Mater. Chem. A 7 (1), 97–106.

Zhang, Z., Wang, H., Sun, J., Guo, K., 2021. Cotton fabrics modified with Si@ hyperbranched poly (amidoamine): their salt-free dyeing properties and thermal behaviors. Cellulose 28 (1), 565–579.